A dynamic energy management system using smart metering

Nsilulu T. Mbungu[a,b,*], Ramesh C. Bansal[b], Raj M. Naidoo[a], Maamar Bettayeb[b,c], Mukwanga W. Siti[d], Minnesh Bipath[e]

[a]Department of Electrical, Electronic and Computer Engineering, University of Pretoria, Pretoria, South Africa
[b]Department of Electrical Engineering, University of Sharjah, Sharjah, United Arab Emirates
[c]Center of Excellence in Intelligent Engineering Systems (CEIES), King Abdulaziz University, Jeddah, Kingdom of Saudi Arabia
[d]Department of Electrical Engineering, Tshwane University of Technology, Pretoria, South Africa
[e]SANEDI: Smart Grids, Johannesburg, South Africa

*Corresponding author at: Department of Electrical, Electronic and Computer Engineering, University of Pretoria, Pretoria, South Africa. ntmbungu@ieee.org

Highlights

• Formulates linear and quadratic model of smart home energy coordination for the intelligent microgrid application.
• Designs optimal energy flow control strategies by the use of a smart metering system based on wireless communication.
• Compares the dynamic performance of the energy management schemes based on demand response.
• Provides the consumer with an opportunity of selling the energy to the utility for a microgrid connected to the main grid.
• Applies system analysis on the energy components of a residential home.

Abstract

Smart grid technologies are a catalyst for the modernisation of the electrical system whilst satisfying all electrical power stakeholders. The application of intelligent systems results in more flexibility and reliability. This paper presents a dynamic energy management system for a microgrid connected to a grid for residential application. The system models a smart metering system to collect data from different components of the electrical system. A grid-tied photovoltaic and energy storage system model is optimally designed. The model uses the framework of a smart grid based on demand response and energy pricing to coordinate the energy flow of a home. Three optimal control scenarios are formulated, where the opportunity energy is considered to be injected to the main grid. These scenarios are two linear methods (open and closed-loop models) and a quadratic approach based on model predictive control. It was observed that the energy storage system plays an essential role in the context of energy-saving and gain from the demand side. The models provide benefits in terms of energy-saving and energy cost. The performance of dynamic modelling is validated with the experimental data from the smart metering system.

Graphical abstract

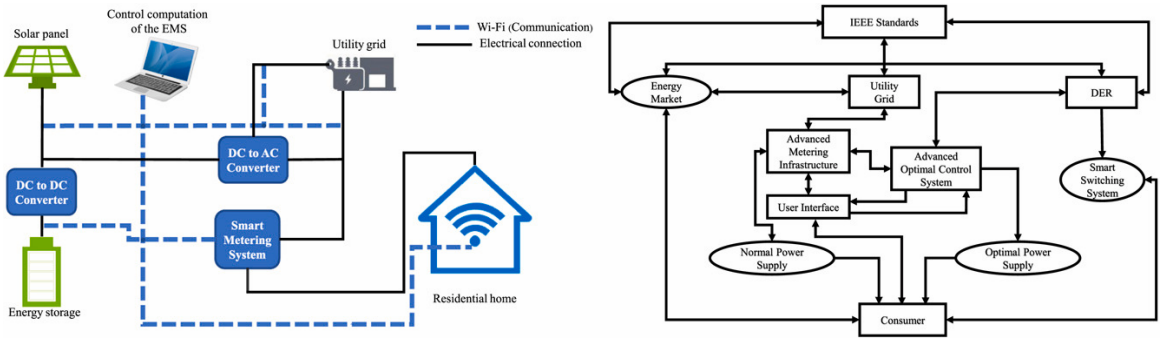

Keywords

Battery energy storage system; Energy efficiency; Grid integration; Smart grid; Solar energy; Utility supply

Nomenclature

Parameters and constants

AC	Alternative current
AMI	Advanced metering infrastructure
BESS	Battery energy storage system
CC	Control computation
CL	Closed-loop
CV	Control variable
DC	Direct current
DEG	Distributed energy generation
DER	Distributed energy resources
DES	Distributed energy storage
DG	Distributed generation
DR	Demand response
DSM	Demand side management
EMS	Energy management system
ESS	Energy storage system
EV	Electric vehicle
GSM	Global system mobile
IEEE	Institute of Electrical and Electronics Engineers
MPC	Model predictive control
MV	Manipulated variable
OP	Open-loop
PI	Proportional–integral
PV	Photovoltaic
RER	Renewable energy resource
RES	Renewable energy system
RTP	Real-time price
SMS	Smart metering system
Wi-Fi	Wireless fidelity

Indices

bat	Battery
c	Control
ch, cha, 5	Charging, input from battery charging
CL	Closed-loop
d	Demand
$d.avrg$	Hourly average energy demand
dis, $disc$, 3	Discharging, input from battery discharging
der	Real-time signal from DER
h	Predicted
i	Initial or given bus of the network
inv	Inverter
j	Sampling of time control
gr	Grid
l	Load
max	Maximum of the signal
min	Minimum of the signal
OL	Open loop

$op, 4$	Opportunity, input from the opportunity
$pv, 1$	Photovoltaic, input from the PV
rw	Renewable energy
$ug, 2$	Utility grid, input from the utility grid
Variables	
Δ	Variation [–]
η	Efficiency [–]
A	State matrix [–]
B	Input matrix [–]
C	Output matrix [–]
$Cost$	Cost [Rand]
CB	Battery capacity [kWh]
D	Feed forward matrix [–]
DOD	Depth of discharge of ESS [–]
E	Energy [kWh]
Ha	Hours of autonomy of the BESS [h]
I	Hourly solar irradiation incident [kW/m^2]
J	Performance index [Rand] and/or [–]
m	Number of inputs [–]
n	Rank of matrix or number of constraints [–]
N	Time horizon of the system [h]
p	Price (real-time pricing) [Rand/kWh]
q	Number of outputs [–]
R	Reference [Rand] and/or [–]
S	Section or surface [m^2]
SOC	State of charge of the ESS [–]
t	Sampling of time [h]
u	Input of the system [kWh]
x	State vector [–]
y	Output [Rand]

1. Introduction

The architectural evolution of the metering assists in the electrical network to unpack new features of coordinating the power flow in real-time for the benefit of all energy stakeholders. The genealogy tree of measuring the power flow in the electrical system is currently being revolutionised by the generation of intelligent grid technologies, which introduce the smart metering system (SMS) [1], [2], [3], [4]. This innovation is based on the development of the advanced metering infrastructure (AMI). The SMS has modernised the traditional power grid by introducing a real-time bi-directional power monitoring system. Several energy management opportunities have been created through the SMS for power network applications with excellent monitoring of the power flow in the electrical system [5].

The energy revolution is dependent on the features of smart grid technologies and assists in the integration of renewable energy resources (RERs) into the electrical grid. The energy management system (EMS), in the framework of smart grids, creates an opportunity for both the consumer and supplier of electricity to operate efficiently for an improved electrical system. The energy storage system (ESS) plays an essential role in the operational process of the EMS when the RERs are integrated into the grid [6], [7], [8], [9], [10]. The ESS has also improved the operation of an isolated electrical system which is only supplied by RERs. The application of a small microgrid, namely nanogrid or picogrid in the residential sector usually requires the use of photovoltaic (PV), which has an ESS and can operate either in grid-connected or islanded mode. The application of SMS allows the energy system of a pico/nanogrid or residential home to be effectively coordinated for improved performance of distributed energy resources (DERs) on the electrical network [5]. One of the best applications for the AMI within the EMS is demand response (DR).

There are several types of DR programs for EMS, namely contracted response, price-based DR and incentive-based DR [5]. DR can provide opportunities for ancillary services [11] and reliability for maintaining the electrical system during extreme events [12]. Several research works present and apply the benefits of the DR in the electrical system [13], [14], [15], [16], [17]. An optimisation based load and DER scheduling method is designed through the use of an improved Nash-equilibrium-based game-theoretic framework for demand side management (DSM) to coordinate the energy flow of the electrical system in [18]. This method was established by combining two DR programs, namely a real-time price (RTP) retail tariff model based on historical and predicted wholesale prices and direct load control. It was observed that the simulation of the developed algorithm resulted in a reduction of peak demand.

The RTP model allows consumers to monitor the cost of energy consumption in real-time [19]. Zhang et al. [20] proposed a novel price strategy that can deal with power volatility on total energy production cost. The proposed method uses a decentralised demand response scheme. The model explores the possibility of reducing the volatility and peak-to-valley difference of aggregated load cure. The designed model was based on a RTP environment. This strategy was also adaptable to scenarios where the RERs could be integrated. The main objective of peer-to-peer electricity trading pricing, which is driven by its benefits to both prosumer and consumer, is assessed in [21]. The conceptual framework of the developed model was implemented for a microgrid with a PV system in a residential sector. The economic feasibility of the energy system was evaluated and

optimal energy trading strategy among all stakeholders of the energy system was established. The proposed model applied a DR scheme through the use of RTP to increase profits.

Park et al. [22] developed a convex optimisation under DR program for a residential home. The model applied smart grid technologies to reformulate the nonconvex problem as a convex to ensure an optimal solution that can maximise user convenience. As the optimisation model is designed by the DR scheme, the mathematical formulation of the system model is developed through DR-based two price policies, namely RTP and progressive approach. Therefore, a heuristic algorithm is developed to obtain an optimal solution from the approximated near-optimal solution for a given nonconvex problem. It was observed that the developed model could also be implemented with the integration of RERs. In [23], an optimal energy dispatch problem was formulated for household energy management using DR. The proposed strategy was designed to combine two different levels, distributed generation (DG) and RTP-based load control and storage-based energy dispatch. The developed model ensures cost-effective energy coordination by the use of a DSM application. The system used wind power and solar panel as DG. The proposed model can meet the end-user's requirements and reduce the electricity costs from the utility grid.

A novel energy management based on real-time and long-term predictions of the solar energy system and load demand is proposed in [24]. The performance of the proposed EMS aims to coordinate energy distribution and analyse the cost of a microgrid. The control system used predictive dynamic programming to manage the energy flow for residential application optimally. The quasi microgrid topology based on a fuzzy controlled energy management unit that can select the appropriate operation mode is respectively designed in [25] and [26]. These models consider the real-time and long-term data to coordinate the energy generation and consumption. A fuzzy-logic controller was selected due to its simplicity to design a comprehensive and intuitive EMS for a large microgrid and its simple linguistic rules that do not require complex mathematical modelling.

In [27], the energy management of a smart home used a quasi configuration for DG, grid integration and DR based RTP. The proposed model offered the end-user an opportunity to sell energy to the main grid under an optimal control strategy. The flexibility of the designed model enabled the coordination of different DER and satisfies the consumer requirements of minimising the energy cost from the utility grid and the energy payback opportunity from the utility grid. In [28], a closed-loop model based on DR through the use of dynamic energy and RER

integration was developed. The proposed model used a proportional–integral (PI) control to formulate a control-theoretic of the energy market management. Through the applied dynamic approach, the difference between the demand and RER was resolved by controlling the elastic demand and measuring the generation of renewable energy.

The dynamic energy management system is effective when it is implemented in a smart grid [29]. This methodology aims to coordinate the energy flow of several power generation components that contain RER and battery energy storage system (BESS) [30], [31]. The proposed system in [32] has the possibility to handle the model uncertainty from the input signal of the DG and/or utility grid, due to the integration of BESS. In [33], the uncertainty of the forecasted parameters can be managed with a robust convex optimisation using the Monte Carlo simulation method for EMS. The model predictive control (MPC) is considered as one of the best techniques of formulating a dynamic EMS. The MPC can effectively cope with data uncertainties in real-time [34]. This structure can be implemented in an open or closed-loop scheme. In [35], a dynamic model for MPC energy management based DR is developed. The designed formulation was under a closed-loop structure for a hybrid system. Detailed research work identified an essential gap in terms of payback energy cost opportunity for the end-user. This paper is, therefore, an advanced model of [27], [35] for a residential application where the SMS is used as an input to the EMS under DR based real-time electricity pricing. The designed approach uses a linear methodology to develop two control schemes, namely open and closed-loop model and the MPC controller to formulate a closed-loop plan through a quadratic equation. The system constitutes four main components. These are the utility grid to supply energy to the load and DER that has three parts of the system. The DER contains Distributed energy generation (DEG) (PV), distributed energy storage (DES) or ESS and end-user. The PV and BESS are the two principal components of DER. It is essential to note that in some scenarios the end-users can be considered as part of DER while in other scenarios they cannot.

The key technical contributions made in this research work can be summarised as follows:

- Use the SMS's feature to optimally determine the power flow of different quadrants of a residential home in real-time.
- Use the strategy to develop the optimal energy management of an intelligent microgrid for residential power consumption.

- Design an optimal switching strategy to control different components of a microgrid through the use of the DR scheme based on a real-time pricing environment.
- Validate the designed models through real data from the intelligent measurement of a residential home.

The remaining part of this research study can be summarised as follows: Section 2 presents the system description of the microgrid. Section 3 presents modelling based on all different system scenarios. Section 4 assesses the system and provides the computation structures of all scenarios. Section 5 depicts different results and discussions. Section 6 presents the conclusion and proposes future research.

- Design an optimal switching strategy to control different components of a microgrid through the use of the DR scheme based on a real-time pricing environment.
- Validate the designed models through real data from the intelligent measurement of a residential home.

The remaining part of this research study can be summarised as follows: Section 2 presents the system description of the microgrid. Section 3 presents modelling based on all different system scenarios. Section 4 assesses the system and provides the computation structures of all scenarios. Section 5 depicts different results and discussions. Section 6 presents the conclusion and proposes future research.

2. System description

It is not feasible to discuss RERs, ESSs and energy efficiency based on active management without smart grid technologies [5]. The microgrid provides the essence of systems thinking through the combination of several components of a DER for improved power flow into the electrical system [36]. Fig. 1 presents a detailed description of a microgrid operation. This structure is considered as a model for energy management of a microgrid for the consumer and the supplier of electric power [5]. This relationship can be summarised as follows:

- When the utility supplier operates in microgrid environment without considering any single relationship with the consumer, the need to have an incredible resilience of that isolated system leads to the loss of reliability of the electrical system, as shown in Fig. 1(a). The necessity of having a reliable

system can cause the entire system to lose its resilience, as explained in Fig. 1(b).

- For a microgrid operating as an islanded microgrid, as shown in Fig. 1(c), i.e. disconnected from the utility grid, the need for end-users to have a more reliable system reduces the resilience of the given power system. Conversely, if consumers opt for greater resilience of the islanded microgrid system, the reliability of the system is reduced. This is caused by the uncertainty and resource constraints associated with RERs.
- A microgrid connected to the main grid provides the electrical system with excellent reliability and resilience that assist to achieve the power system's operational objectives of satisfying both the supplier and consumer of the energy Fig. 1(d).
- The research study aims to investigate the system behaviour based on microgrid goals, as depicted in Fig. 1. The system operates by integrating the DER (PV and ESS) to the grid for residential applications based on intelligent home energy management.

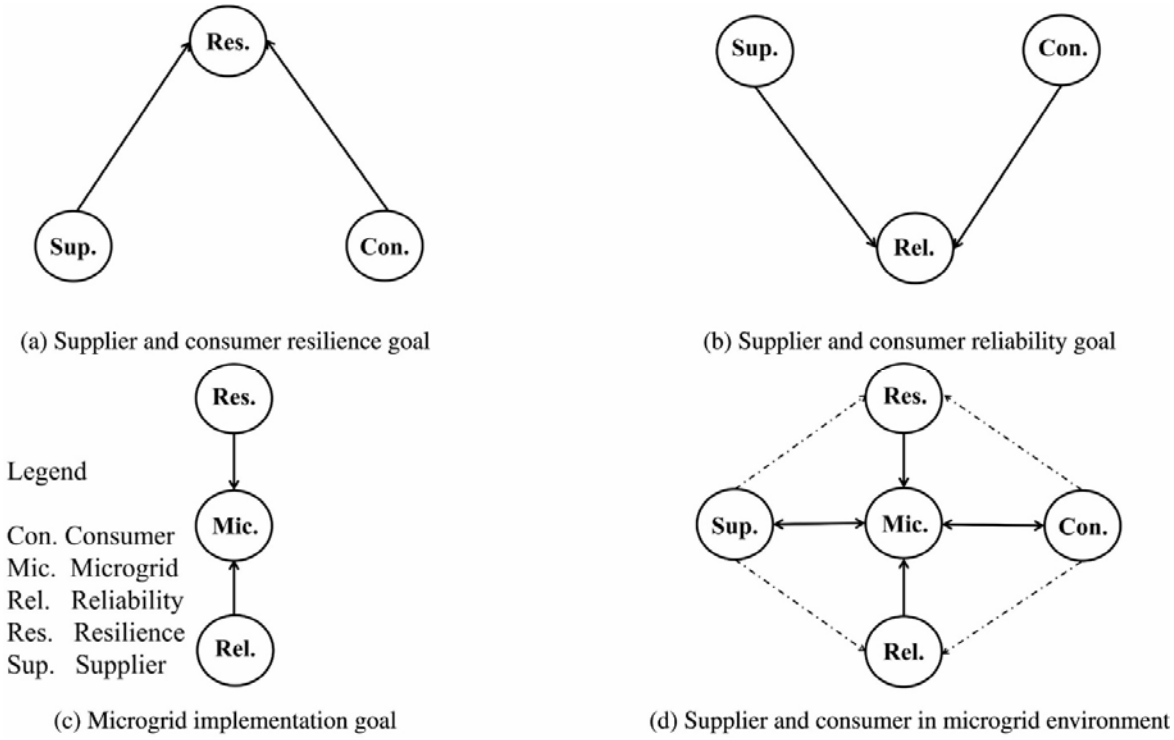

(a) Supplier and consumer resilience goal

(b) Supplier and consumer reliability goal

(c) Microgrid implementation goal

(d) Supplier and consumer in microgrid environment

Fig. 1. Microgrid goals: the relationship between supplier and consumer.

2.1. System layout

Fig. 2 presents an intelligent microgrid connected to the main grid for residential application. It constitutes PV solar, ESS and utility grid to supply the power demand of one home. The SMS provides an opportunity to collect the real-time data of different energy generation components (PV, BESS and utility grid) of the system. The communication of the network between the SMS and the optimal switching of control computation (CC) model under EMS is based on wireless fidelity (Wi-Fi). The model identifies the optimal behaviour of the system which gives the consumers the opportunity to minimise the energy cost from the grid and to maximise the energy from DER. Through the EMS philosophy for the microgrid, as detailed in Fig. 1, the system operates in a manner that guarantees the reliability and resilience of the entire electrical grid.

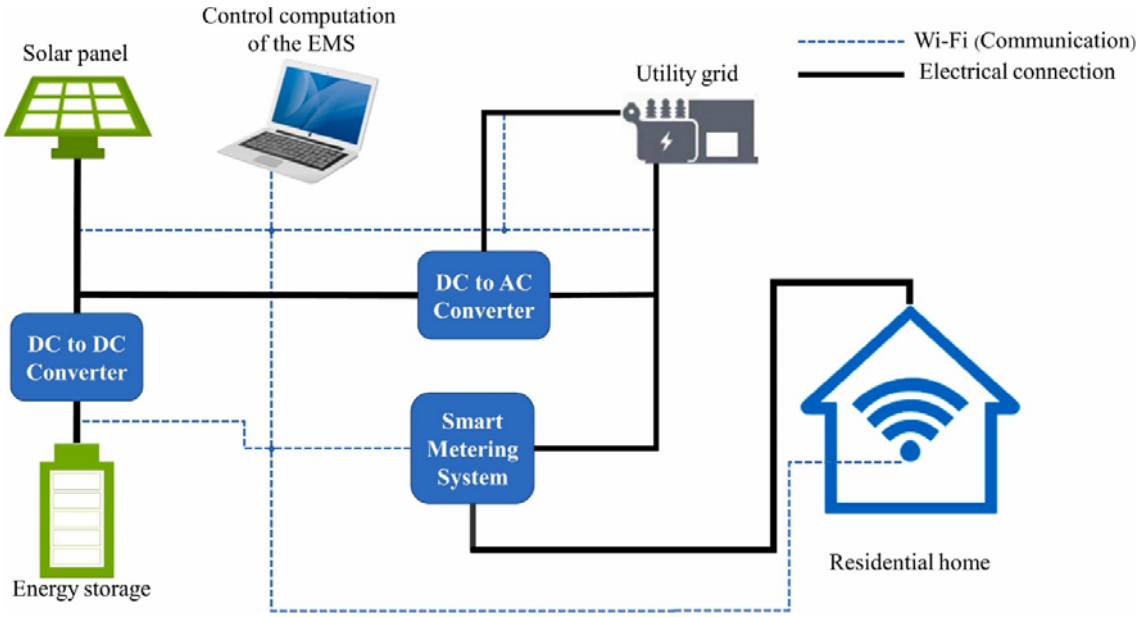

Fig. 2. Smart microgrid for residential energy management system.

2.2. System distributed energy resource

The EMS for the microgrid requires accurate measurement of the energy generation from different DER (PV and BESS). The energy from the solar panel is a function of solar irradiation. The BESS uses a dynamic model based on either the energy flow on the battery or state of charge (SOC) of the ESS. Eq. (1) describes the time series of the energy generated from the solar panel [37], [38], [39].

$$E_{pv}(t) = \eta_{pv} A_{pv} \Delta t \sum_{t=1}^{N} I_{pv}(t) \quad (1)$$

where I_{pv} is the solar irradiation incident measured on the PV panel [kW/m^2], t is the time [h], N is the sampling time of the time series [h], Δt is the time variation [h], A_{pv} is the PV panel surface [m^2], and η_{pv} is the PV panel efficiency.

In this paper, the dynamic model of battery is formulated through the SOC of the ESS. Therefore, the dynamic model of the SOC of the battery is formulated as [27]:

$$\mathrm{SOC}\,(t+1) = \mathrm{SOC}\,(t) - \frac{E_{dis}(t)}{\eta_{dis}\eta_{inv}CB} + \frac{E_{ch}(t)\eta_{ch}}{\eta_{inv}\,\mathrm{CB}} \tag{2}$$

where E_{dis} is the discharging energy from the battery [kWh], E_{ch} is the energy to charge to the battery [kWh], η_{dis} is the discharging efficiency of the ESS, η_{ch} is the charging efficiency of the BESS, η_{inv} is the inverter efficiency of the ESS, and CB is the capacity of the BESS [kWh], which is determined by:

$$\mathrm{CB} = \frac{\mathrm{Ha}\;E_{d.avg}}{\eta_{inv}\eta_{dis}\;\mathrm{DOD}} \tag{3}$$

where Ha, $E_{d.avg}$ and DOD are the hours of autonomy of the BESS [h], the average of the energy demand [kWh/h] based on time series of the horizon N and depth of discharge of BESS respectively. DOD is formulated by:

$$\mathrm{DOD}\,(t) = 100 - \mathrm{SOC}\,(t) \tag{4}$$

Eq. (4) shows that the capacity of the BESS, as detailed Eq. (3), can vary as a function of the time, which also affects Eq. (2). This variation demonstrates that the capacity of BESS has a minimal, nominal and maximal value which depend on the SOC of battery.

2.3. Utility grid

The energy flow from the main grid to the load is under dynamic electricity pricing from the utility grid. Eq. (5) details the discrete dynamic model of the energy cost system based on real-time electricity pricing. This model can be computed for the energy generation system, either renewable or conventional power generation. The SMS assists in the computation of Eq. (5) [19].

$$Cost_{gr}\,(t+1) = Cost_{gr}\,(0) + p_{gr}\,(t)\,E_{gr}\,(t) \tag{5}$$

where $Cost$, p_{gr} and E_{gr} are the energy cost [Rand], the real-time electricity price [Rand/kWh] and energy supply from the utility grid [kWh].

3. Model description and development

The energy management of the designed system communicates through a Wi-Fi based on global system mobile (GSM) to share data from the SMS to the control scheme in real-time. This Section describes the development of the control schemes.

3.1. Model description

Fig. 3 presents a detailed model of the microgrid system as detailed in Fig. 2. Through this structure, the system energy flow can be expressed as follows:

$$E_{ut}(t) = E_{gr}(t) \tag{6}$$

$$E_{PV}(t) = E_{pv.l}(t) + E_{ch}(t) \tag{7}$$

$$E_{bat}(t) = E_{dis}(t) + E_{ch}(t) \tag{8}$$

$$E_l(t) = E_{pv.l}(t) + E_{gr}(t) + E_{disc}(t) \tag{9}$$

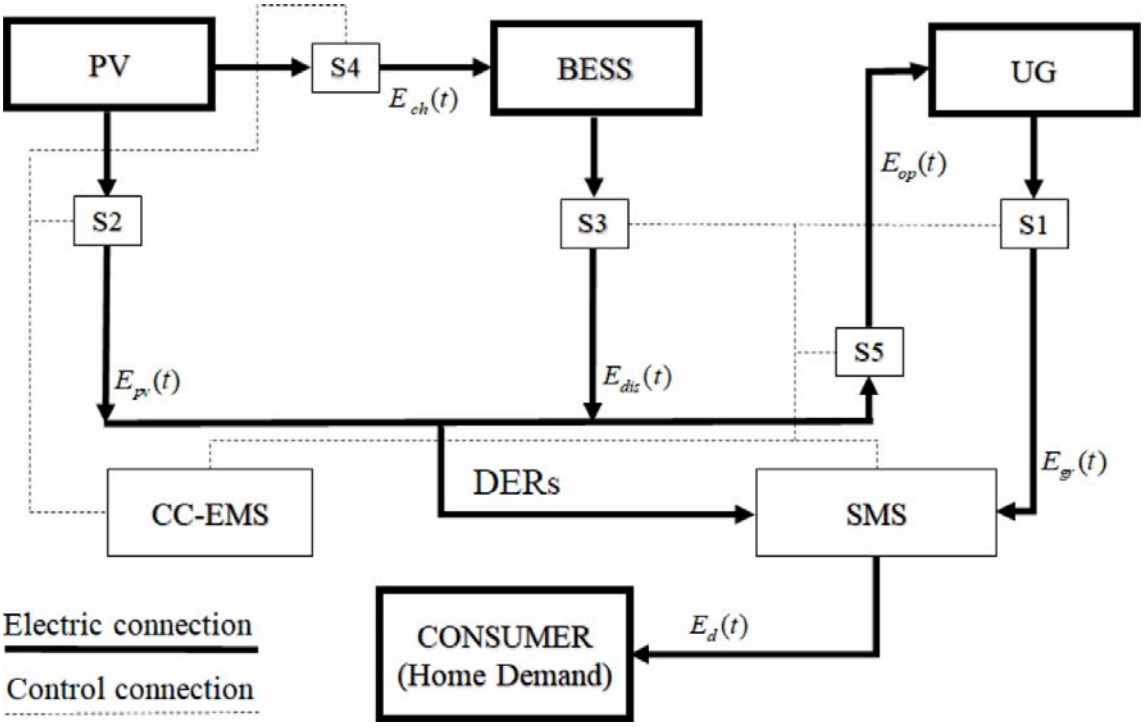

Fig. 3. Residential microgrid system connected to the grid for EMS.

where E_{ut} is the supplied energy by the utility grid [kWh], $E_{pv.l}$ is the energy from the PV to supply the load [kWh], E_l is the energy demand [kWh] , and E_{bat} is the energy flow on the BESS [kWh]. The discharging energy of the battery as described in Eq. (2) has two parts, namely the energy to supply the load and the energy sold to the grid. This is expressed as follows:

$$E_{dis}\,(t) = E_{disc}\,(t) + E_{op}\,(t) \tag{10}$$

where E_{disc} is the energy from the battery to supply the load [kWh], E_{op} is the opportunity energy to sell to the utility grid [kWh]. Based on Eqs. (2), (10) and the limitations of ESS developed in [32], [40], the energy drawn on the battery developed in Eq. (8) can be expressed during the charging and discharging process respectively:

$$\begin{bmatrix} E_{bat_{cha}}\,(t) \\ E_{bat_{dis}}\,(t) \end{bmatrix} = \begin{bmatrix} E_{cha}\,(t) & 0 \\ 0 & E_{disc}\,(t) + E_{op}\,(t) \end{bmatrix} \tag{11}$$

where $E_{bat_{cha}}$ and $E_{bat_{dis}}$ is the energy on the battery during the charging [kWh] and discharging [kWh] process. Eq. (11) is also considered as the battery constraints to avoid charging and discharging at the same time.

The input matrix of the designed system can be formulated through the analysis of the model description as expressed in Fig. 3 and from Eqs. (6) to (10). The control variables (CVs) of the microgrid system is a function of the energy flow in each component as described in Eq. (12).

$$[\,u\,(t)\,] = [\,E_1\,(t) \quad E_2\,(t) \quad E_3\,(t) \quad E_4\,(t) \quad E_5\,(t)\,]^T \tag{12}$$

where $u\,(t)$ is the system input matrix [kWh], $E_1\,(t) = E_{pv.l}\,(t)$, $E_2\,(t) = E_{gr}\,(t)$, $E_3\,(t) = E_{disc}\,(t)$, $E_4\,(t) = E_{op}\,(t)$, and $E_5\,(t) = E_{cha}\,(t)$. From Eq. (12), it is shown that the load demand does not directly affect the input of the system, but it is used to model the system behaviour of CVs. Thus, if it assumed the system is constituted of the controllable and non-controllable loads as developed in [41], [42], [43], this can be effectively handled by the system modelling.

3.2. Open-loop EMS

The open-loop model aims to find an optimal solution of the input matrix of Eq. (12). For a given time horizon of the system computation, it is assumed that the control horizon is equated to the system horizon. The model performance index is a function of the output of the system or manipulated variables (MVs) of the designed system. From Eq. (5), the initial value of the energy cost ($Cost\,(0)$) in most scenarios is equated to zero. When it is assumed that $Cost\,(0) > 0$, Eq. (13) can be verified.

$$Cost_{gr}\,(0) = Cost_{gr}\,(t) \tag{13}$$

The discrete model developed in Eq. (5) can be written as a function of Eq. (13) and the CV of the utility grid can be defined in Eq. (12) as:

$$Cost_2\,(t+1) = Cost_2\,(t) + p_{gr}\,(t)\,E_2\,(t) \tag{14}$$

Where $Cost_2$ is the utility electricity cost that the consumer pays to the DSO.

The same method, as way developed in Eq. (14), can be used for other MVs, the designed system can be expressed as follows:

$$Cost_1\,(t+1) = Cost_1\,(t) + p_{rw}\,(t)\,E_1\,(t) \tag{15}$$
$$Cost_3\,(t+1) = Cost_3\,(t) + p_{rw}\,(t)\,E_3\,(t) \tag{16}$$
$$Cost_4\,(t+1) = Cost_4\,(t) + p_{rw}\,(t)\,E_4\,(t) \tag{17}$$
$$Cost_5\,(t+1) = Cost_5\,(t) + p_{rw}\,(t)\,E_5\,(t) \tag{18}$$

where $Cost_1$, $Cost_3$, $Cost_4$, $Cost_5$ and p_{rw} are cost of energy supply by the PV [Rand], cost of energy from the ESS to supply the load [Rand], cost of energy from ESS to sell to the utility grid [Rand], cost of energy from the PV to charge the battery [Rand] and the real-time electricity price from renewable energy resources [Rand/kWh] respectively. From Eqs. (14) to (18), the MVs matrix can be written as:

$$[\,y\,(t)\,] = [\,Cost_1\,(t) \quad Cost_2\,(t) \quad Cost_3\,(t) \quad Cost_4\,(t) \quad Cost_5\,(t)\,]^T \tag{19}$$

where $y\,(t)$ is the output matrix of the open-loop system [Rand].

The objective function of the designed model is to maximise the use of DERs and minimise the energy from the utility grid. Considering a given time horizon N_h of the system and linear expression of the output matrix as presented in Eq. (19) with system objective function, the performance index can be expressed as:

$$\min\ J_{OL}\,(t) = \sum_{t=1}^{N_h} [Cost_2\,(t) - (Cost_1\,(t) + Cost_3\,(t) + Cost_4\,(t) + Cost_5\,(t))] \tag{20}$$

where J_{OL} is the performance index of the open-loop system [Rand].

3.3. Closed-loop EMS

When the control horizon N_c is different from the predicted time or output horizon N_h, the closed-loop model can be described. The closed-loop scheme objective function is written as:

$$\min\ J_{CL}\,(t) = \sum_{t=1}^{N_h} \sum_{j=1}^{N_c=t} \big[Cost_{2.t_j}\,(t) - \big(Cost_{1.t_j}\,(t) + Cost_{3.t_j}\,(t) + Cost_{4.t_j}\,(t) + Cost_{5.t_j}\,(t)\big)\big] \tag{21}$$

3.4. Model predictive control EMS

The control scheme uses MPC. The objective function derives from a quadratic design of the state space model. This is expressed as follows [37]:

$$\begin{bmatrix} x(t+1) \\ y(t) \end{bmatrix} = \begin{bmatrix} A & B \\ C & D \end{bmatrix} \begin{bmatrix} x(t) \\ u(t) \end{bmatrix} \tag{22}$$

where $x(t)$ is the state vector, A is the state matrix, B is the input matrix, C is the output matrix, and D is the feed forward matrix or disturbance matrix.

The designed system, as described in Fig. 2, Fig. 3, depends on combining energy flow from different system components. These are detailed in Eqs. (6), (9). Through this design approach, the system model aims to be identified with the dynamic model, expressed in Eq. (2). The dynamic model of the utility grid is reformulated in Eq. (14). It is also worth noting that the energy flow on the demand-side is assumed to be DER which does not generate any energy. The cost of energies from the DER as the energy flows are detailed from Eqs. (7) to (9) can be written as a function of the system CVs described in Eq. (12) as:

$$Cost_{pv}(t+1) = Cost_{pv}(t) + p_{rw}(t)\left(E_1(t) + E_5(t)\right) \tag{23}$$
$$Cost_{bat}(t+1) = Cost_{bat}(t) + p_{rw}(t)\left(E_3(t) + E_4(t) + E_5(t)\right) \tag{24}$$
$$Cost_l(t+1) = Cost_l + p_{rw}(t)\,E_1(t) + p_{gr}(t)\,E_2(t) + p_{rw}(t)\,E_3(t) \tag{25}$$

where $Cost_{pv}$ is the cost of energy on the PV generation [Rand], $Cost_{bat}$ cost of energy on the BESS [Rand] and $Cost_l$ cost of consumption energy [Rand].

The state vector of the MPC design is a function of Eqs. (2), (14) to (23), (24), (25), and it is expressed as follows:

$$[x(t)] = [\mathrm{SOC}(t) \quad Cost_{gr}(t) \quad Cost_{pv}(t) \quad Cost_{bat}(t) \quad Cost_l(t)]^T \tag{26}$$

Through the state vector, Eq. (26), and the designed state–space model of Eq. (22), the state matrix can be formulated as:

$$A = I_n \tag{27}$$

where I_n is an identity matrix of $n \times n$, with $n = 5$ which is the number of the states of the system model and also the number of the CVs variables of the system defined in Eq. (12). Based on the system model as described in Section 3.1 and from Eqs. (22) to (27), the input matrix of the MPC design is expressed as follows:

$$B(t)=\begin{bmatrix} 0 & 0 & \frac{-1}{CB(t)\eta_{disc}\eta_{inv}} & \frac{-1}{CB(t)\eta_{disc}\eta_{inv}} & \frac{\eta_{ch}}{CB(t)\eta_{inv}} \\ 0 & p_{gr}(t) & 0 & 0 & 0 \\ p_{rw}(t) & 0 & 0 & 0 & p_{rw}(t) \\ 0 & 0 & p_{rw}(t) & p_{rw}(t) & p_{rw}(t) \\ p_{rw}(t) & p_{rw}(t) & p_{rw}(t) & 0 & 0 \end{bmatrix} \tag{28}$$

From Eqs. (22) to (28), the output matrix of the state–space model can be written as:

$$C = I_n \tag{29}$$

Eq. (29) shows that the output matrix of the designed system is the same as the state matrix. Therefore, the output vector of the MPC design is the same as the state vector presented in Eq. (26). This system identification shows that the MV vector of the linear open and closed-loop scheme, as detailed in Eq. (19), is different from the output vector of the MPC design, which can be expressed as:

$$[y(t)]=[\mathrm{SOC}(t) \quad Cost_{gr}(t) \quad Cost_{pv}(t) \quad Cost_{bat}(t) \quad Cost_{l}(t)]^T \tag{30}$$

The MPC performance index of the EMS system is determined by:

$$\min\ J_{MPC}(t)=\sum_{t=1}^{N_h}\sum_{j=1}^{N_c=t}\left(y_{t_i}(t)-R_{t_i}(t)\right)\left(y_{t_i}(t)-R_{t_i}(t)\right)^T \tag{31}$$

where $R(t)$ is the system reference in which the model should track. For a given time t of the predicted time horizon or system time horizon N_h and the control horizon sample $j=t$, the MV vector as described in Eq. (31) is determined by:

$$y(t)=Fx(t)+\Phi(t)u(t) \tag{32}$$

with $F(t)=\begin{bmatrix} CA & CA^2 & \cdots & CA^{N_h} \end{bmatrix}^T$, and

$$\Phi(t)=\begin{bmatrix} CB(t) & 0 & \cdots & 0 \\ CAB(t) & CB(t) & & 0 \\ \vdots & \vdots & \ddots & \vdots \\ CA^{N_h-1}B(t) & CA^{N_h-2}B(t) & \cdots & CA^{N_h-N_c}B(t) \end{bmatrix}.$$

Eq. (31) presents a performance index of a quadratic function for the MPC. The designed structure of both open and closed-loop scheme has a linear model of the objective function, as described in Eqs. (21) and (20).

3.5. System constraints

The system constraint of the control schemes derives from the CVs, MVs, designed limitations, state vector and the increment of the input signal. It is important to note that the constraint matrix depends on the system inputs constraints. Table 1 summarises the impact of the system constraints for each designed model, namely open-loop, closed-loop and MPC. The determination of a maximal number of constraints that can be handled on any designed control system is determined in Eq. (33). This formulation is more applicable for an MPC system design [37], and it can also be set for other control model schemes.

$$n = 4mN_c + 2qN_h \tag{33}$$

where m is the number of inputs and q is the number of outputs of the system design.

Apart from Eqs. (6), (7), (9), (11) which define the constraint matrix of load demand, ESS, PV, utility grid, as presented in Table 1, the CVs, MVs, increment of CV and state vector constraints can be listed as:

$$\begin{cases} M_{1_i} = [-I_i, I_i]^T \\ \gamma_{1_i} = [-E_{min_i}, E_{max_i}]^T \end{cases} \tag{34}$$

$$\begin{cases} M_{2_i} = [-\Phi, \Phi]^T \\ \gamma_{2_i} = [(-Cost_{min_i} + Fx(t)), (Cost_{max_i} - Fx(t))]^T \end{cases} \tag{35}$$

$$\begin{cases} M_{3_i} = [-U_{2_i}, U_{2_i}]^T \\ \gamma_{3_i} = [(\Delta E_{min_i} + U_1 \Delta E_i (k-1)), (\Delta E_{max_i} - U_1 \Delta E_j (k-1))]^T \end{cases} \tag{36}$$

$$\begin{cases} M_{4_i} = [-x_{m_i}, x_{m_i}]^T \\ \gamma_{4_i} = [(x_i(t) - x_{min_i}) L, (x_{max_i} - x_i(t)) L]^T \end{cases} \tag{37}$$

where $i = 1, 2, 3, 4$ and 5, which represent each CV, MV and state vector of the system. The particularity of the MPC design as described in Section 3.4 is that the number of inputs, outputs and state of the system is equated. I and U_2 represent a diagonal identity matrix attached to CV and MV respectively, U_1 is the lower triangular vector and L is an identity vector of control horizon row which is joined to x_{m_i}. The system constraint is the computation of each constraint, as specified in Table 1 depending on a given control scheme. For the open and closed-loop plan, the state constraint that the system may consider is only based on the state of charge of the battery and in its inequality model as described in Table 1. It should be noted that the CVs contain the lower and upper boundaries constraints. The

SOC constraint of the linear model does not have considerable impact on the inequality constraint as compared to the MPC scheme. The computation matrix of the constraint system is represented by [37]:

$$ME(t) \leqslant \gamma \tag{38}$$

where M and γ individually combine all the M_{k_i} and γ_{k_i} where k represents the type of constraint as described in Table 1.

Table 1. Summary of constraints matrix.

Constraint	Type	Open-loop	Closed-Loop	MPC	Equation
Inputs (CVs)	Inequality	✓	✓	✓	Eq. (34)
Outputs (MVs)	Inequality	✗	✗	✓	Eq. (35)
Increment of CV	Inequality	✗	✗	✓	Eq. (36)
State vector	Inequality	✗	✗	✓	Eq. (37)
Load demand	Equality	✓	✓	✓	Eq. (9)
Battery storage	Equality	✓	✓	✓	Eq. (11)
Solar PV supply	Equality	✓	✓	✓	Eq. (7)
Utility grid	Equality	✓	✓	✓	Eq. (6)

4. System analysis and algorithm

Fig. 4 presents the system interaction based on system analysis and systems thinking of the designed model. It shows the relationship of the entire electrical system, as presented in Fig. 3. This is derived from several subsystems and is composed of four main components and some subsystem components. The other parts of the system are the energy market, IEEE standards, smart switching system, optimal control system, and SMS that contains the AMI, user interface and real-time monitoring to depict the non-optimal and optimal results. The relationship of different subsystems permits determination of the interaction of different components of the model. The analysis of different subsystems or components of the system design layout for a grid-integrating DER is the advanced development of Fig. 1, which provides the principal goals of a microgrid's operation.

Through the layout model of the EMS, the computational steps of the system design layout of the microgrid, as depicted in Fig. 4, can be used to describe the implementation algorithm of each scenario. The summary algorithm for all control schemes can be stepped as follows:

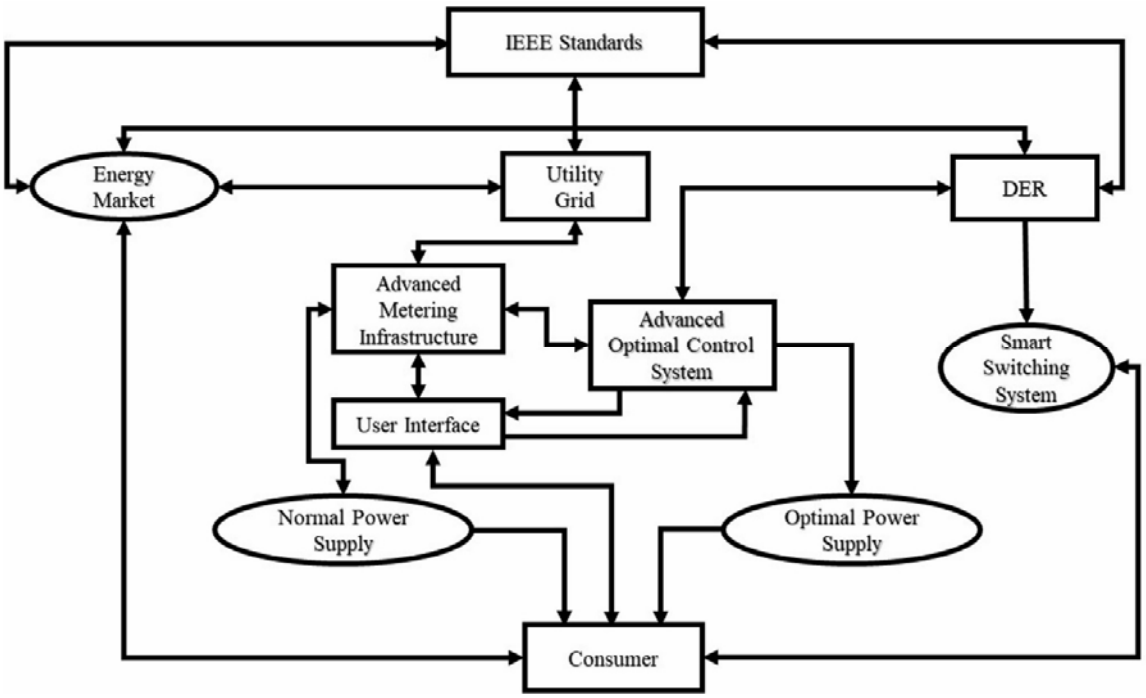

Fig. 4. System design layout: grid-connected DER.

Step 1:

Start the optimal control process for either open or closed-loop or MPC scheme by identifying the CVs.

Step 2:

Set the time horizon of the control structure and/or the control horizon N_c for the closed-loop and MPC model.

Step 3:

Update system parameters at a sample of time. This is chosen to be at $t = i$ where $i = [1..N]$.

Step 4:

Read the energy flows on each component through the SMS as described in Fig. 2, Fig. 3.

Step 5:

Update the system constraints (Eq. (38)) at given time $t = i$ for the computing control scheme (open loop, closed-loop and MPC scheme) based on Table 1 and system performance requirements.

Step 6:

Compute the EMS through the use of SMS strategy based on DR as described in Eqs. (20) or (21) or (31), for open-loop or closed loop or MPC design respectively.

Step 7:

Find the optimal solution of the CVs for either open-loop or closed-loop or MPC scheme. If this solution is not optimal, repeat step 2 to 7 to get the optimal solution.

Step 8:

Generate the optimal solution for open-loop. Update the system control horizon for either closed-loop or MPC scheme, at $t_{updated} = i + 1$.

Step 9:

Repeat the system process for either the closed-loop or MPC control model from step 2 and 9 until the computed model reaches the solution at the specified time horizon.

Step 10:

Generate the optimal solution of the system from closed-loop control or MPC design.

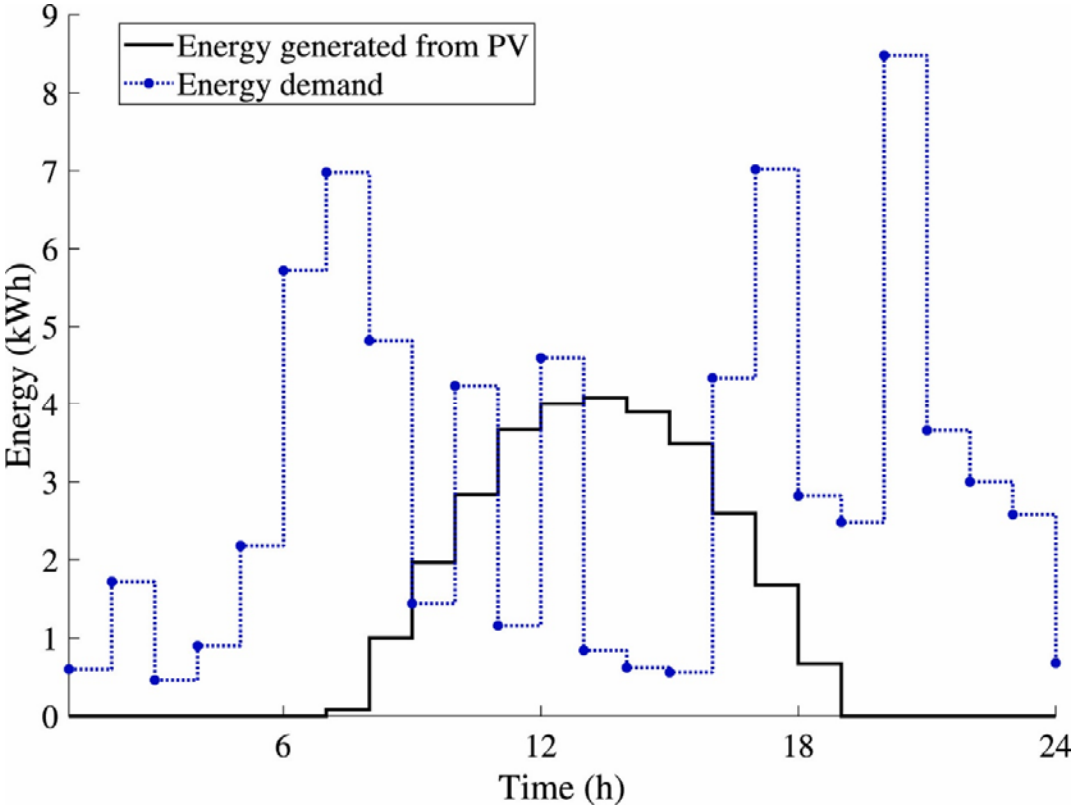

Fig. 5. Daily energy demand and generated energy from PV panel.

5. Simulation of results and discussion

The computation of the system constraints, especially for MPC scheme as presented in Table 1, does not necessarily consider all independent constraints of MVs, state vector and the increment of CVs. The consideration of system constraints depends on the system performance requirements that the MVs have to follow. Fig. 5 depicts the load profile and the forecasting generated power from the PV panel. It is assumed that these data are accurate and without uncertainty. Table 2 provides the computational parameters. The energy price is expressed in Rand/kWh. All minimum values of CVs are set to zero while their maximum values are attached to the peak value of the energy demand.

Table 2. Computation parameters.

Parameters	Values	Parameters	Values
η_{ch}	0.85	SOC_{max}	0.95
η_{disc}	0.95	SOC_{min}	0.40
η_{inv}	0.92	Ha	5
pr_{gr}	1.25	N_h	24
pr_{rw}	0.65	N_c	$[1\ N_h]$

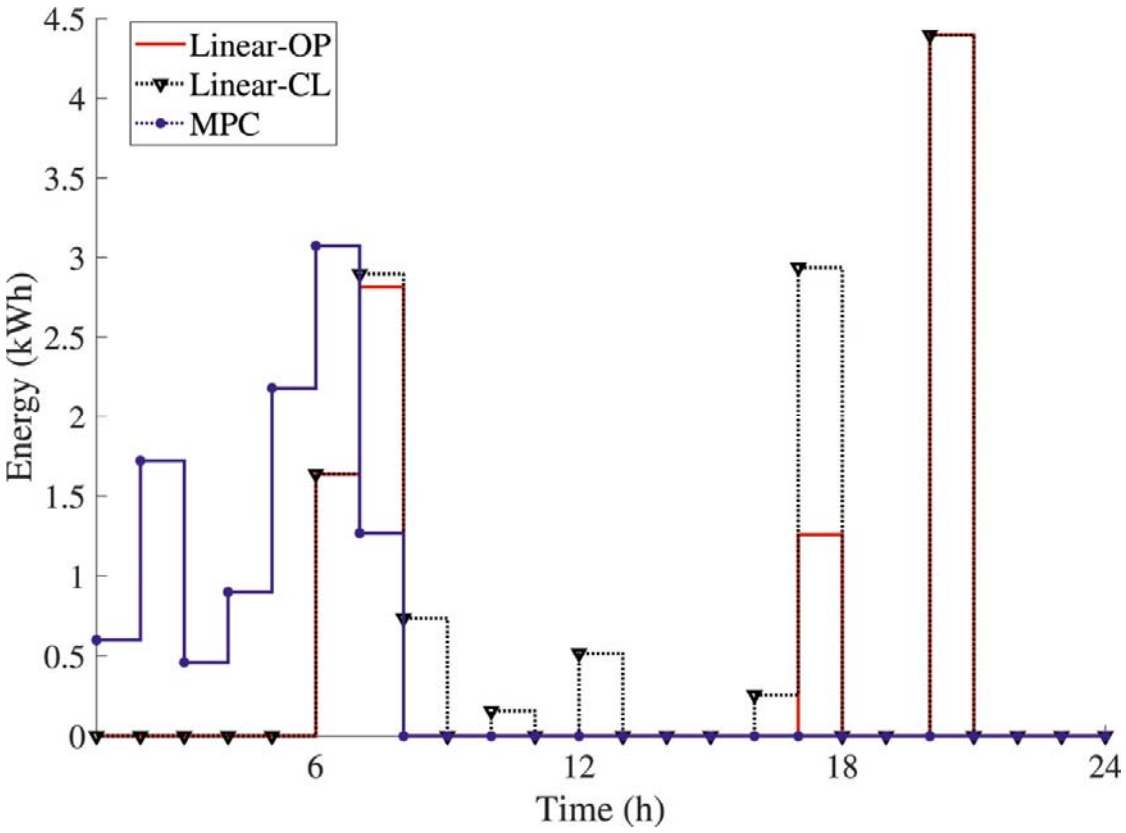

Fig. 6. Energy supply to the load from the utility grid.

5.1. Presentation of the results

Fig. 6, Fig. 7, Fig. 8, Fig. 9, Fig. 10 present the system results of all CVs after the computation of all different scenarios. For open-loop scheme, the control horizon, N_c, is the same as the predicted horizon ($N_p = 24$), as described in Table 2. The closed-loop scheme has different values for control and predicted horizon, and these computation parameters are set to $N_c = 1$ and $N_p = 24$. The MPC scheme based on EMS used the quasi configuration as the closed-loop model setting of $N_c = 2$ and $N_p = 24$. For the MPC, the control horizon, $N_c = 2$, is set based on the optimal selection as described in [35]. All scenarios used the same computation scheme detailed in Table 2. The system computation of all three scenarios use the designed objective function as formulated in Eqs. (20), (21), and (31) respectively. Eq. (31), which formulates the performance index of the MPC scheme shows that the computation structure of these scenarios needs computational reference data. Therefore, the system used the results from the closed-loop model to set the target of the MPC structure.

Fig. 6 depicts the optimal results of the energy consumption from the main grid. As a microgrid system, the energy from DER to supply the end-user is presented in Fig. 7, Fig. 9, both BESS and PV. The implementation of results shows an important minimisation of the energy from the utility grid and maximisation of the energy from the PV and BESS to supply the load demand. Fig. 8 depicts the optimal energy to charge the battery for all three scenarios.

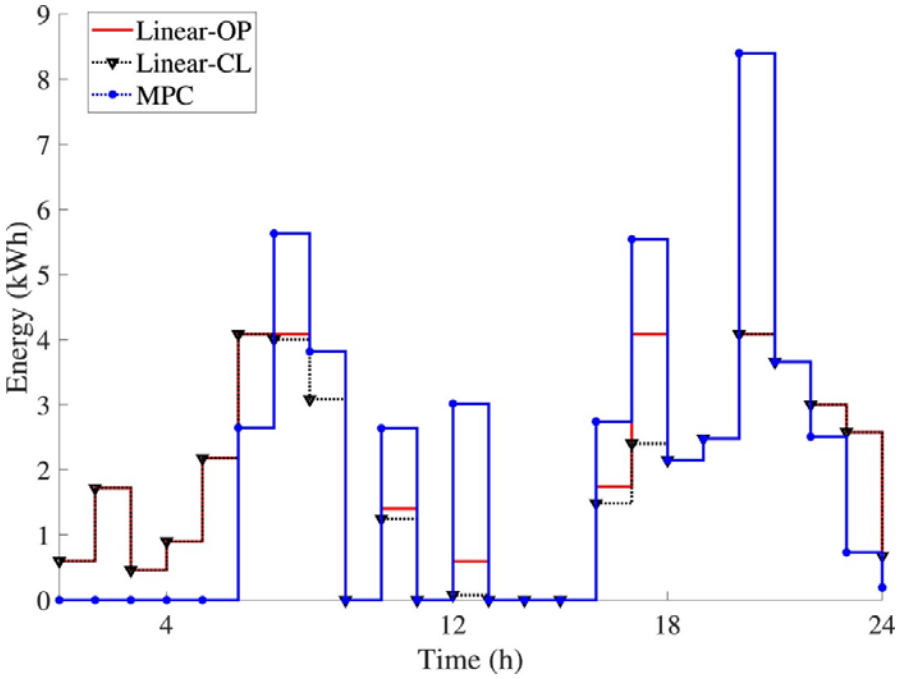

Fig. 7. Energy supply to the load from battery (discharging energy from ESS).

5.2. Discussion of the results

It was observed that the generated energy from the PV to charge the BESS has the same profile for all scenarios, as described in Fig. 8. However, the energy from the discharged battery to supply the end-user, as depicted in Fig. 7, has an important limitation in the morning, a slight difference when the PV is generating, and a quasi great gap in the evening. Fig. 9 shows the quasi reality in terms of having the same profile of generated energy from the PV to supply the demand. For the linear models and quadratic MPC scheme, the energy supplied from the PV panel does not have the same profile. The linear models provide a considerable difference in the energy demand from the PV compared to MPC. While the reference of the system of Eq. (32) depends on the closed-loop model, the MPC model does not depend on the system reference. This is due to the system constraints and parameters, as detailed in Table 1, where the MPC scheme offers the possibility to handle different constraints of the system design. The same observation is also shown in Fig. 6, Fig. 7.

Fig. 10 presents the profiles of the energy opportunity from all scenarios. An important profile of the opportunity from the MPC scheme was observed compared to the open and closed-loop model. This profile has a different pattern from the closed-loop model that is supposed to be the target of the opportunity system for the MPC scenario. It is important to note that the system reference of the MPC model does not directly depend on the CVs of the open-loop model. Although this is computed in the function of the closed-loop scheme, Eq. (30) provides a brief formulation of reference of the MPC controller which derives from Eqs. (2), (23), (24), (25). In addition, the MPC model uses a computation structure where the input matrix, $B(t)$, varies in function of each computation time t as described in Eq. (28). This variation also affects the computation of the performance index as formulated in Eq. (31), which has variable output structure that is detailed in Eq. (32) where $\Phi(t)$ is a function of $B(t)$. This computation formation is different from the MPS based EMS with a quadratic performance index as designed in [37].

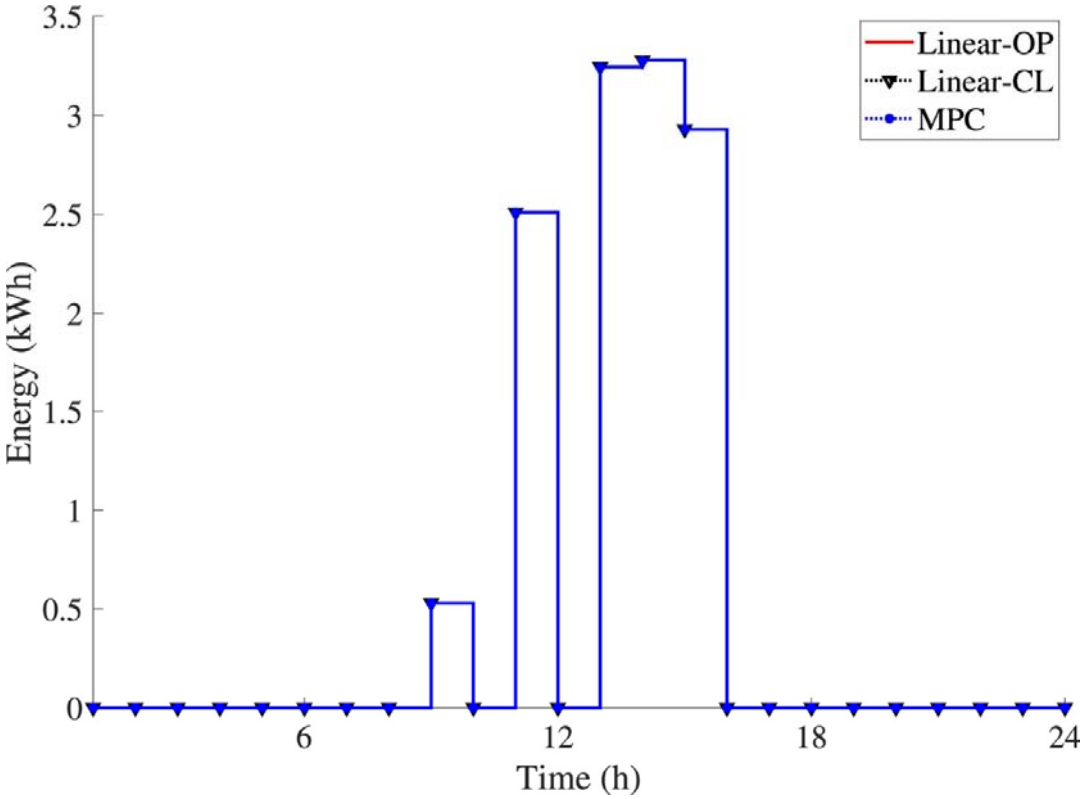

Fig. 8. Energy to charge the battery.

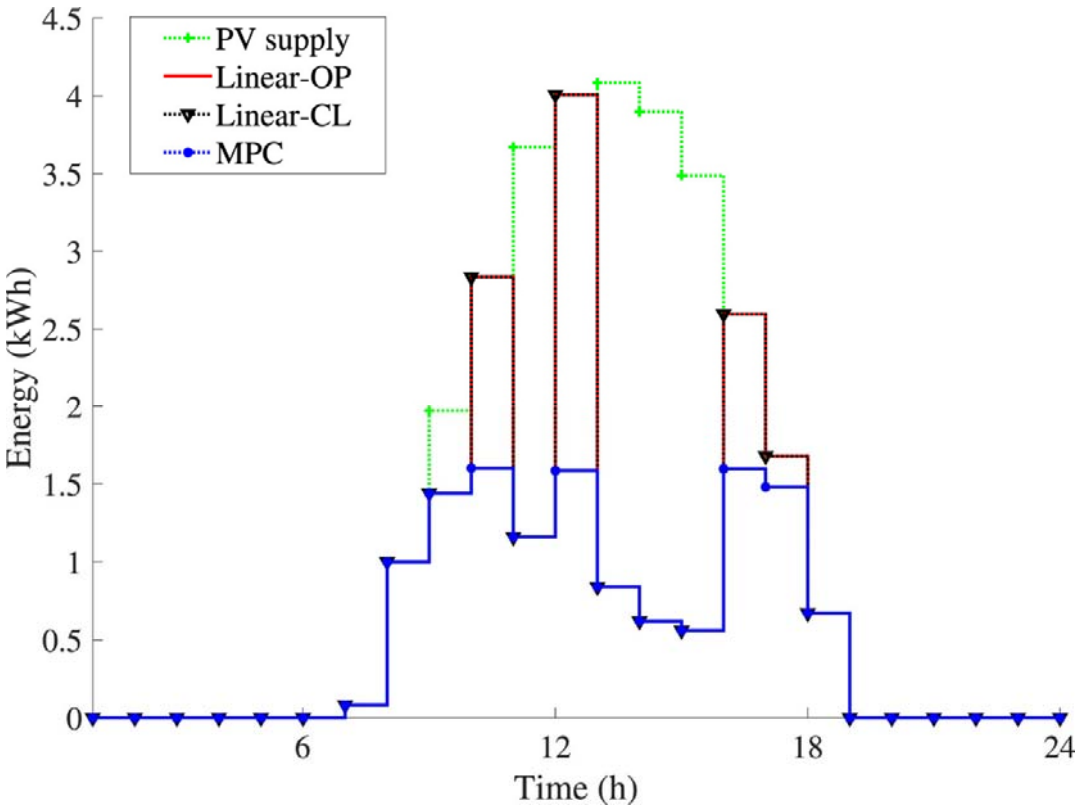

Fig. 9. Energy supply to the load from the PV.

Table 3 represents the computational results of all scenarios. This structure gives the sum of the optimal consumed energy from the utility grid, opportunity energy, payback value in the energy, non-optimal supply and the consumer gain. The non-optimal energy supply is the sum of the load demand when it is assumed that there is no implementation of any control scenario on the system. The payback energy is the difference between the opportunity and the optimal energy from the supply [27]. The consumer gain is the percentage of the energy that the end-user can benefit when the control scenarios are implemented and it is formulated to be the ratio of payback energy by the non-optimal supply. In terms of reference to follow the optimal energy from the utility grid, the open-loop and MPC scheme have roughly the same supplied energy from the main grid. However, the closed-model offers a value that is different from other optimal control schemes. In addition, greater value was observed in MPC opportunity energy as compared to open and closed-loop computation. The MPC also has excellent payback energy that the system can save. The third scenario (MPC) offers a 28% gain while the open and closed-loop provide approximately 21% and 5% gain.

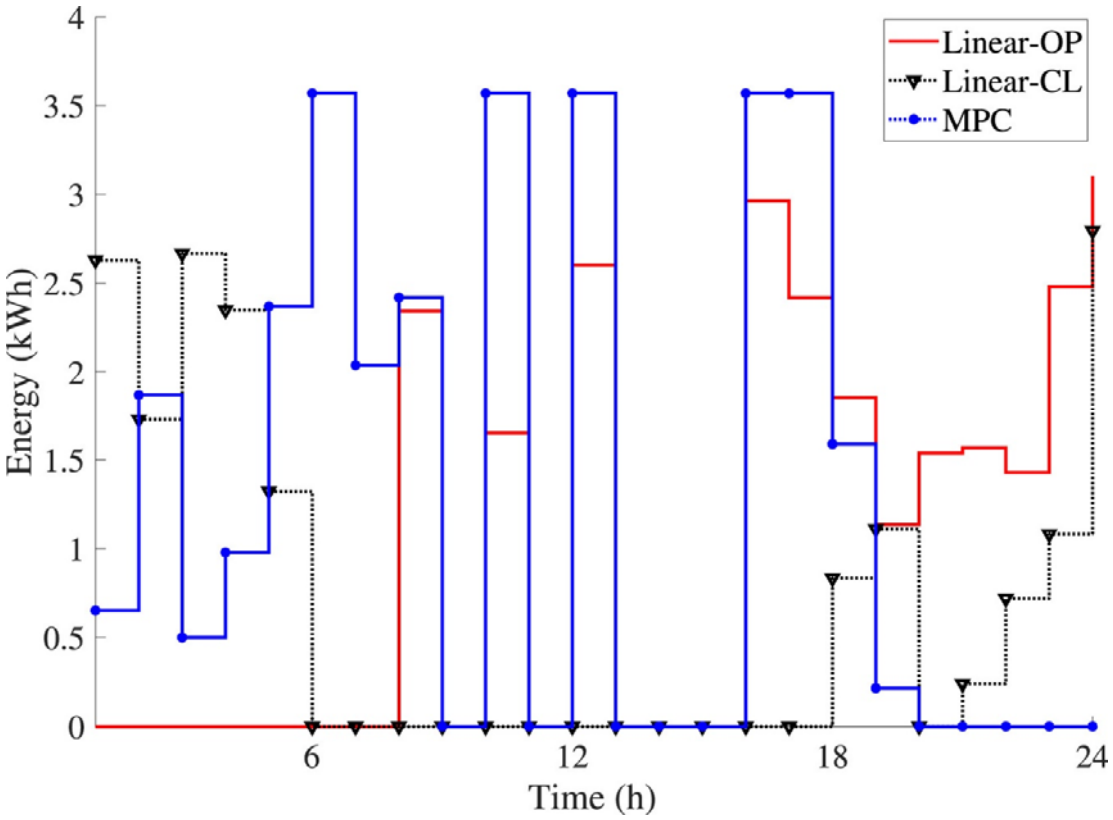

Fig. 10. Opportunity Energy to sell to the utility grid.

Table 3. System energy analysis based on consumer benefits.

Scenarios	Optimal energy supply	Opportunity energy	Payback energy	Non-optimal energy supply	Consumer energy gain
Open-loop scheme	10.11	25.09	14.98	71.9	0.21
Closed-loop scheme	13.53	17.48	3.95	71.9	0.05
MPC scheme	10.20	30.48	20.28	71.9	0.28

When the energy price is considered as described in Table 2, the system cost analysis of all scenarios can be presented. Table 4 shows the energy cost analysis of all methods. This presentation depends on Eqs. (5), (14), (18), where the system is formulated with a real-time electricity pricing that does not vary in function of time and the time series of the energy are summed, as described in Table 2, Table 3 respectively. The gain value thus decreases when it is considered in cost value compared to the energy value, as shown in Table 3. The MPC computation still offers the excellent value of energy cost gain for the consumer, which is 8%. The open-loop model has 4% while the closed-loop provides -6%. It was observed that for the closed-loop scheme, the consumer has to pay about 6% of the total cost of energy demand to the supplier.

Table 4. System cost energy analysis based on consumer benefits.

Scenarios	Optimal supply Cost	Opportunity Cost	Payback Cost	Non-optimal cost supply	Consumer cost gain
Open-loop scheme	12.64	16.31	3.67	89.88	0.04
Closed-loop scheme	16.91	11.36	−5.55	89.88	−0.06
MPC scheme	12.75	19.81	7.06	89.88	0.08

Fig. 11 depicts the dynamic of energy flowing on the battery based on the SOC, as formulated in Eq. (2) with all system implementation variations of the SOC as detailed in Eqs. (3), (4). This outline provides an excellent profile of the energy flowing on BESS for the closed-loop model compared to open and the MPC

development structure. It is essential to note that the system implementation of BESS does not take into consideration the constrained value of Ha, which is set to 5, as shown in Table 2. This computation system uses the hypothesis of maximising the energy flow on the DES in which the BESS can discharge as much as the demand needs to be supplied until it reaches the minimum value of the SOC of battery [44]. A normal BESS that is used in DEG can be continually discharged for more than 24 h or less than 2 days [9], [45], [46]. This depends on the operational usage of BESS as the design system used the PV load. This is often constrained by resource limitation, as shown in Fig. 5. The closed-loop model can perform better in the context of microgrid goals, as depicted in Fig. 1. The open-loop and MPC scheme also achieve the microgrid goals from the first predicted horizon of the computational results. The open-loop also provides the lowest value at the end of SOC profile that can reach the minimum, as shown in Fig. 11. For the MPC scheme which provides more opportunity of the energy and cost, as detailed in Table 3, Table 4, there is an opportunity to increase the system gain. This problem can be resolved by adjusting the maximum value of the increment of the input constraint and/or input constraint of the opportunity energy (E_4). It was observed that opting for a battery with the lowest minimum value of SOC can resolve this problem for both open-loop and MPC scheme.

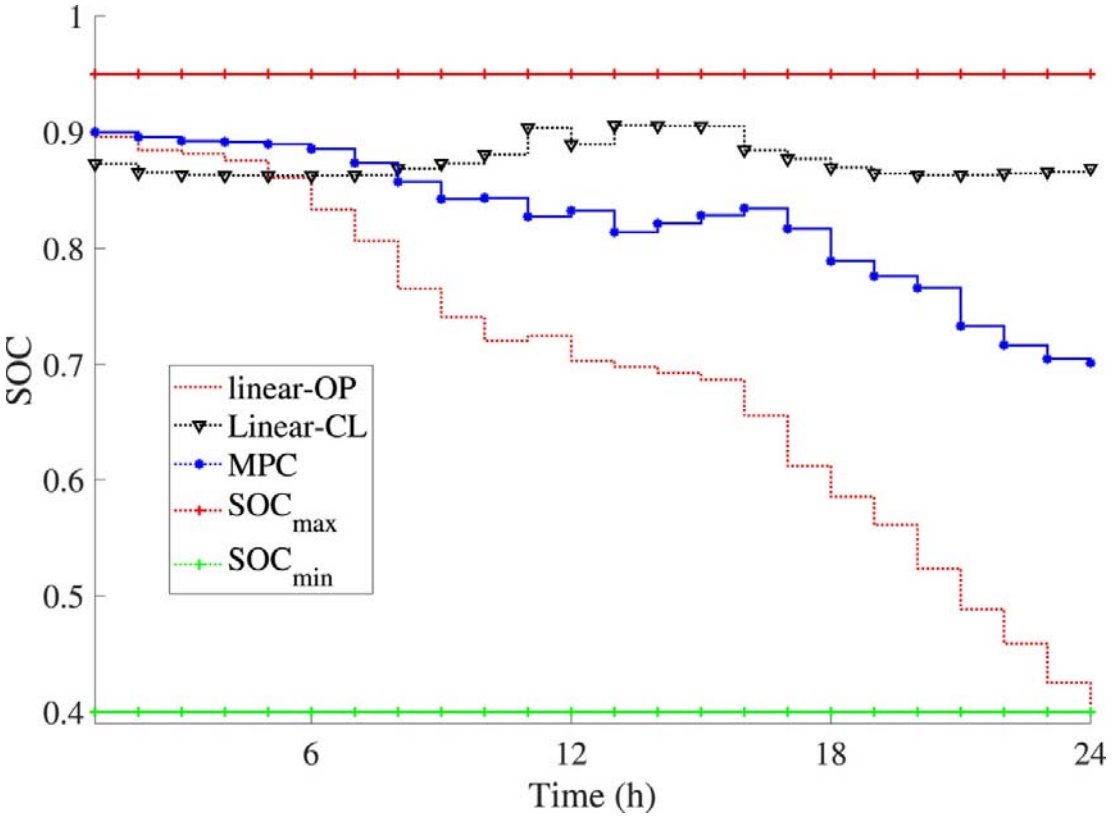

Fig. 11. Time series of SOC of battery.

6. Conclusion

The dynamic modelling of an energy management system has several design options. These methodologies can improve the power flow of a given electrical system and offer diverse opportunities to both the supplier and consumer of electrical power. Intelligent metering allows for the implementation of energy management strategies. In this paper, three scenarios of the dynamic energy management system were formulated to coordinate the energy flow of a smart microgrid for a residential application. The developed approaches use the demand response based price under the real-time electricity pricing structure to manage the microgrid. This consists of a grid integrating distributed energy generation and storage. A smart home energy management model was designed to compute all optimal control scenarios through system analysis. It was observed that the formulated strategies provide a better energy gain to the consumer. This gain is a result of the opportunity energy that the end-user can inject to the primary grid. This assists the consumer to achieve up to 28% of the total energy consumption. Through the energy cost analysis, the cost gain on the demand-side could reach approximately 8%, which is less than the energy gain. This decrease in the value of energy cost gain is due to the lower amount of price from the distributed energy generation. The distributed energy storage also played an essential role in energy-saving for all designed approaches. The closed-loop scheme provided an outstanding performance of the dynamic model due to the profile of the state of charge of battery with a negative value of cost gain. The model predictive control offered an excellent improvement in the context of energy-saving as compared to both linear strategies with a lower state of charge of the energy storage that can be fixed by the system constraints. This could also be resolved with the lowest minimal value of the state of charge and the lower maximal value of the input of opportunity constraint and/or increment of the opportunity constraints.

Future research works will explore the implementation of the energy policies for smart home implementation. The research will also be based on developing approaches in terms of the power quality to be injected into the main grid and the value of opportunity energy and energy cost gain for the benefit of all energy stakeholders.

CRediT authorship contribution statement

Nsilulu T. Mbungu: Conceived and designed the analysis, Collected the data, Contributed data or analysis tools, Performed the analysis, Project administration, Writing - original draft Writing - review & editing. **Ramesh C. Bansal:**

Conceived and designed the analysis, Collected the data, Contributed data or analysis tools, Performed the analysis, Wrote the paper, Writing - review & editing. **Raj M. Naidoo:** Conceived and designed the analysis, Collected the data, Contributed data or analysis tools, Performed the analysis, Wrote the paper, Writing - review & editing. **Maamar Bettayeb:** Conceived and designed the analysis, Contributed data or analysis tools, Performed the analysis, Wrote the paper, Writing - review & editing. **Mukwanga W. Siti:** Conceived and designed the analysis, Contributed data or analysis tools, Performed the analysis, Wrote the paper. **Minnesh Bipath:** Conceived and designed the analysis, Contributed data or analysis tools, Performed the analysis, Wrote the paper.

Declaration of Competing Interest

The authors declare that they have no known competing financial interests or personal relationships that could have appeared to influence the work reported in this paper.

Acknowledgements

The authors thank the Smart grids Lab and Power Group at the University of Pretoria, South Africa, National Research Foundation, South Africa, and University of Sharjah, UAE , for financial and other support.

References

[1] Olivares-Rojas JC, Reyes-Archundia E, Gutiérrez-Gnecchi JA, González-Murueta JW, Cerda-Jacobo J. A multi-tier architecture for data analytics in smart metering systems. Simul Model Pract Theory 2019;102024.
[2] Mbungu N, Naidoo R, Bansal R, Bipath M. Grid integration and optimization through smart metering. In: 2nd SAIEE Smart Grid Conf., Midrand, South Africa; 2017. p. 19–21.
[3] Weranga K, Kumarawadu S, Chandima D. Smart metering design and applications. Heidelberg, Germany: Springer; 2014.
[4] Toledo F. Smart metering handbook. PennWell Books; 2013.
[5] Mbungu NT, Naidoo RM, Bansal RC, Vahidinasab V. Overview of the optimal smart energy coordination for microgrid applications. IEEE Access 2019; 7:163063–84.
[6] Ajanovic A, Hiesl A, Haas R. On the role of storage for electricity in smart energy systems. Energy 2020;117473.
[7] Zhang X, Lovati M, Vigna I, Widén J, Han M, Gal C, et al. A review of urban energy systems at building cluster level incorporating renewable-energy-source (RES) envelope solutions. Appl Energy 2018; 230:1034–56.
[8] Bansal RC. Handbook of distributed generation: electric power technologies, economics and environmental impacts. Cham, Switzerland: Springer; 2017.
[9] Mbungu NT, Naidoo RM, Bansal RC, Siti MW, Tungadio DH. An overview of renewable energy resources and grid integration for commercial building

applications. J Energy Storage 2020; 29:101385.
[10] Rahbar K, Xu J, Zhang R. Real-time energy storage management for renewable integration in microgrid: An off-line optimization approach. IEEE Trans Smart Grid 2015;6(1):124–34.
[11] Wang H, Wang S, Tang R. Development of grid-responsive buildings: Opportunities, challenges, capabilities and applications of HVAC systems in non-residential buildings in providing ancillary services by fast demand responses to smart grids. Appl Energy 2019; 250:697–712.
[12] Wang F, Xu H, Xu T, Li K, Shafie-Khah M, Catalão JP. The values of market-based demand response on improving power system reliability under extreme circumstances. Appl Energy 2017; 193:220–31.
[13] Palensky P, Dietrich D. Demand side management: Demand response, intelligent energy systems, and smart loads. IEEE Trans Ind Inform 2011;7(3):381–8.
[14] Samad T, Koch E, Stluka P. Automated demand response for smart buildings and microgrids: The state of the practice and research challenges. Proc IEEE 2016;104(4):726–44.
[15] Mbungu NT. Dynamic real time electricity pricing optimisation for commercial building. [Master's thesis], South Africa: University of Pretoria; 2017.
[16] Strbac G. Demand side management: Benefits and challenges. Energy Policy 2008;36(12):4419–26.
[17] Gellings CW. The concept of demand-side management for electric utilities. Proc IEEE 1985;73(10):1468–70.
[18] Fernandez E, Hossain M, Nizami M. Game-theoretic approach to demand-side energy management for a smart neighbourhood in Sydney incorporating renewable resources. Appl Energy 2018; 232:245–57.
[19] Mbungu NT, Naidoo RM, Bansal RC. Real-time electricity pricing: TOUMPC based energy management for commercial buildings. Energy Procedia 2017; 105:3419–24.
[20] Zhang Z, Li F, Shi H. A pricing strategy reflecting the cost of power volatility to facilitate decentralized demand response. IEEE Access 2019;7: 105863–71.
[21] An J, Lee M, Yeom S, Hong T. Determining the peer-to-peer electricity trading price and strategy for energy prosumers and consumers within a microgrid. Appl Energy 2020; 261:114335.
[22] Park L, Jang Y, Cho S, Kim J. Residential demand response for renewable energy resources in smart grid systems. IEEE Trans Ind Inf 2017;13(6):3165–73.
[23] Yang Q, Fang X. Demand response under real-time pricing for domestic households with renewable DGs and storage. IET Gener Transm Distrib 2017;11(8):1910–8.
[24] Jafari M, Malekjamshidi Z, Zhu J. A magnetically coupled multi-port, multioperation-mode micro-grid with a predictive dynamic programming-based energy management for residential applications. Int J Electr Power Energy Syst 2019; 104:784–96.
[25] Jafari M, Malekjamshidi Z, Zhu J, Khooban M-H. Novel predictive fuzzy logic-based energy management system for grid-connected and off-grid operation of residential smart micro-grids. IEEE J Emerg Sel Top Power Electron 2018; 8:1391–404.
[26] Jafari M, Malekjamshidi Z, Lu DD-C, Zhu J. Development of a fuzzy-logic-based energy management system for a multiport multioperation mode residential smart microgrid. IEEE Trans Power Electron 2019;34(4):3283–301.
[27] Mbungu NT, Bansal RC, Naidoo R. Smart energy coordination of autonomous residential home. IET Smart Grid 2019;2(3):336–46.
[28] Kaygusuz A. Closed loop elastic demand control by dynamic energy pricing in smart grids. Energy 2019; 176:596–603.

[29] Aktas A, Erhan K, Özdemir S, Özdemir E. Dynamic energy management for photovoltaic power system including hybrid energy storage in smart grid applications. Energy 2018; 162:72–82.
[30] Ghasemi A, Shayeghi H, Moradzadeh M, Nooshyar M. A novel hybrid algorithm for electricity price and load forecasting in smart grids with demand-side management. Appl Energy 2016; 177:40–59.
[31] Buayai K, Chinnabutr K, Intarawong P, Kerdchuen K. Applied MATPOWER for power system optimization research. Energy Procedia 2014; 56:505–9.
[32] Sperstad IB, Korpås M. Energy storage scheduling in distribution systems considering wind and photovoltaic generation uncertainties. Energies 2019;12(7):1231.
[33] Giraldo JS, Castrillon JA, López JC, Rider MJ, Castro CA. Microgrids energy management using robust convex programming. IEEE Trans Smart Grid 2018;10(4):4520–30.
[34] Hosseini SM, Carli R, Dotoli M. A residential demand-side management strategy under nonlinear pricing based on robust model predictive control. In: 2019 IEEE International conference on systems, man and cybernetics. IEEE; 2019, p. 3243–8.
[35] Mbungu NT, Bansal RC, Naidoo RM. Dynamic energy management strategy under price-based demand response scheme. In: International conference on applied energy. Västerås, Sweden; 2019. Aug 12–15.
[36] Adefarati T, Bansal RC. Reliability, economic and environmental analysis of a microgrid system in the presence of renewable energy resources. Appl Energy 2019; 236:1089–114.
[37] Mbungu NT, Bansal RC, Naidoo R, Miranda V, Bipath M. An optimal energy management system for a commercial building with renewable energy generation under real-time electricity prices. Sustainable Cities Soc 2018; 41:392–404.
[38] Apichonnabutr W, Tiwary A. Trade-offs between economic and environmental performance of an autonomous hybrid energy system using micro hydro. Appl Energy 2018; 226:891–904.
[39] Ogunjuyigbe A, Ayodele T, Akinola O. Optimal allocation and sizing of PV/Wind/Split-diesel/Battery hybrid energy system for minimizing life cycle cost, carbon emission and dump energy of remote residential building. Appl Energy 2016; 171:153–71.
[40] Carli R, Dotoli M, Jantzen J, Kristensen M, Othman SB. Energy scheduling of a smart microgrid with shared photovoltaic panels and storage: The case of the Ballen marina in Samsø. Energy 2020; 198:117188.
[41] Ziadi Z, Taira S, Oshiro M, Funabashi T. Optimal power scheduling for smart grids considering controllable loads and high penetration of photovoltaic generation. IEEE Trans Smart Grid 2014;5(5):2350–9.
[42] Mbungu NT, Naidoo RM, Bansal RC, Bipath M. Smart SISO-MPC based energy management system for commercial buildings: technology trends. In: IEEE future technologies conference. San Francisco, CA, USA; 2016. p. 750–53.
[43] Hosseini SM, Carli R, Dotoli M. Robust day-ahead energy scheduling of a smart residential user under uncertainty. In: 2019 18th European control conference. IEEE; 2019, p. 935–40.
[44] Masoumi A, Ghassem-zadeh S, Hosseini SH, Ghavidel BZ. Application of neural network and weighted improved PSO for uncertainty modeling and optimal allocating of renewable energies along with battery energy storage. Appl Soft Comput 2020; 88:105979.
[45] Lopes D, Sarmento H. Powering an autonomous offshore monitoring buoy. Renew

Energ Offshore 2015;313–8.
[46] Keck F, Lenzen M, Vassallo A, Li M. The impact of battery energy storage for renewable energy power grids in Australia. Energy 2019; 173:647–57.